

Structural Behavior of a Wing in Deformable Ground Effect of a Seaplane

Anjaly Jose, Sheeja Janardhanan, Ajith Kumar Arumugham-Achari, Rajesh P Nair

Abstract: *The study of different age people from different lifestyle, what all symptoms came for the disease, at what stage, what measures taken to get rid of, later changes, what were the side effects, how it decreased or increased will help in future prediction of possible chance for illness in others. A System which having the above details, suggestions from good and expert practitioners, can be used to give warnings to people about the possibility to get affected after 5 or 10 years and to take pre-cautions . Combinational outcome of Descriptive, Predictive and Prescriptive Data Analytics methods on past and present structured and unstructured Big Data can be used to predict future after effects which should be prioritized and treated. Suggestions can be given to people to take appointment with dieticians, change food habits, perform exercises, practice remedial measures etc. Right step at correct time save lives, gives happiness to families, reduces medical expenditures. The relevant information hidden in massive amount of data are made available by the AI assistants to make better clinical decisions in the functional areas of healthcare. To make such a system, a detailed study on big data, analytics methods, health care, practicing methods, electronic health records etc is required. A preventive guidance and less cost expert system which is helpful for common man and experts, for immediate solution and care can be developed in future. Deep machine learning algorithms to detect later possibility of occurrence should be developed. For this a study on Big Data and Health Care Analytics is done.*

Index Terms: *Big Data, Data Analytics, Descriptive Analytics, Predictive Analytics, Prescriptive Analytics, Volume, Velocity, Veracity.*

I. INTRODUCTION

Seaplanes are powered fixed wing aircraft capable of taking off and landing on water. They are completely independent of regular land based airfields. Seaplanes needs sturdy hull, so that they are heavier than conventional aircraft. Because of producing more drag seaplanes have both lower rate-of-climb and cruising speed than conventional aircraft of same power [1]. The flight envelope for a seaplane mostly involves flying close to the surface of the water.

Wing-in-Ground (WIG) craft which flies close to the water surface on a dynamic air cushion of high pressure created by aerodynamic lift due to the ground effect between the vessel and the water surface. Due to its close proximity to the surface

Revised Manuscript Received on December 22, 2018.

Anjaly Jose Department of Civil Engineering SCMS School of Engineering & Technology, Karukutty, Ernakulam.

Sheeja Janardhanan, Department of Mechanical Engineering, SCMS School of Engineering & Technology, Karukutty, Ernakulam.

Ajith Kumar Arumugham-Achari Department of Mechanical Engineering Rajagiri School of Engineering & Technology, Kakkannad, Ernakulam, India.

Rajesh P Nair, Department of Ship Technology Cochin University of Science and Technology, Kochi, Ernakulam.

of water, they have large lift to drag ratio (L/D) which means WIG craft has an increased aerodynamic efficiency and this is the ground effect (GE) phenomenon [2].

Extensive operation of seaplanes can bring down the cost of building airports [3]. The aerodynamic and hydrodynamic interaction of wing is an important aspect that should be considered during WIG design. As the craft is in straight afloat condition, the weight of the craft is supported by water through buoyancy, as the craft speeds up the hydrodynamic drag builds up and reaches a maximum point which is called Hump Drag. At faster speed, the aerodynamics lift becomes significant enough to lift the seaplane and thus the hydrodynamic drag starts to reduce gradually up to the take-off point [4].

In the present paper the seaplane is considered as a WIG craft. WIG effect studies for seaplanes vary in that the ground here is a deformable boundary offered by the free surface of water [3]. So that the aero-hydrodynamic characteristics of wing has to be studied. The lift-to-drag ratio should be maximum for the effective operation of the seaplanes. WIG effect for seaplanes will help in reducing time, effort, and money of the conventional marine transportation in the future [2]. A seaplane under WIG effect is shown in Fig 1.



Fig. 1 A seaplane under WIG effect

Computational fluid dynamics (CFD) simulations and towing tank test experiments have to be carried out to investigate the hydrodynamics of a WIG aircraft. M. Mobasher Tofa et al. conducted an experimental investigation of a Wing-in-Ground (WIG) effect craft and the results show a new proposed design of the WIG craft with compound wing and endplates, which can clearly increase the aerodynamic efficiency without compromising the longitudinal stability. B.C. Khoo & H.B. Koe, conducted a towed-tank test experiment as well as computational fluid dynamics



simulation to investigate the hydrodynamics of a WIG craft. Mohammad Tavakoli & Mohammad Sareed Seif, presented a fast, economical and practical method for mathematical modeling of aerodynamic characteristics of rectangular wing-in-ground effect (WIG) [5].

The objective of this work is to study the aero-hydrodynamics interaction when wing moves in close proximity to the surface of the water by employing computational fluid dynamics simulations. This study would provide the optimum height to chord length (h/c) ratio on the lift-to-drag ratio for a symmetrical airfoil. The structural analysis of the wing has been carried out under a uniformly distributed load (UDL) on the wing obtained from CFD computations. From static structural analysis, the compression and tension in the fibers, total deformation, Von Mises stress, also known as equivalent stress, shear stress, maximum principal stress, maximum shear stress and stress intensity induced in the wing have been computed by considering the wing as a cantilever beam. The results have also been compared from the analytical expressions from the theory of flexural bending.

II. MODELING

A. Computational Domain

2D model of the wing and the surrounding air-water domain was created to find out the free-surface deformations and undulations for different values of h/c . Computational domain should be carefully selected for the simulations and the boundaries should be far off to exclude any undesired numerical reflections. It also should be computationally economical. Here the domain boundaries are chosen in the range $15c$ for inlet and $5c$ for outlet longitudinally, and laterally to the top and bottom it is $6c$. Fig. 2 represents the computational domain.

B. Grid Generation

The maximum cell in the inner domain is $0.01c$ and on the wing it is $0.005c$. This is based on the Balsius theory for boundary layer thickness on flat plates. In the outer domain the maximum cell size is $0.1c$. The cell size used in the air-water interface is same as that used in the boundary layer. Here an overset grid method which is a proven meshing technique for handling forward velocities without elemental distortion. The inner mesh and outer mesh are superimposed one over the other [6] to obtain the wing forward motion. Geometric modeling and meshing have been carried out using ANSYS ICEM CFD (version 18.1). 2D quadrilateral elements have been used to mesh the domain. The meshed computational domain for the present simulations is as shown in Fig 3.

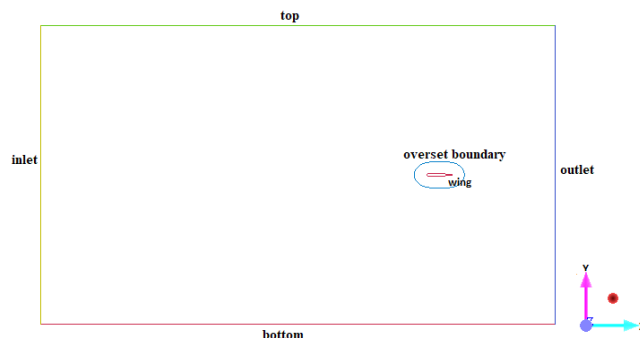
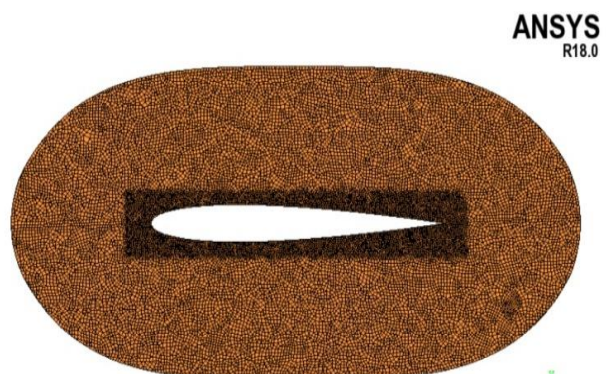


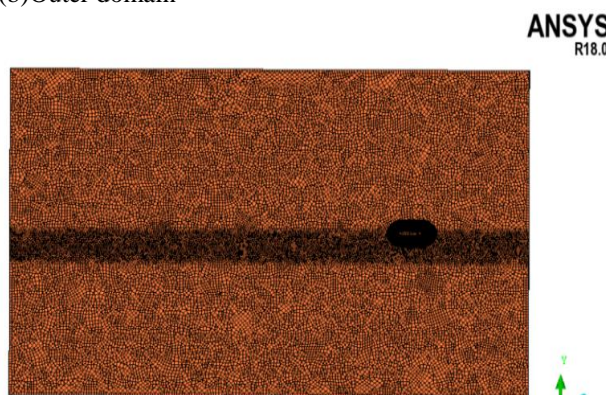
Fig. 2 Computational domain



(a) Inner domain



(b) Outer domain



(c) Overset grid

Fig. 3 Meshed diagram

III. SIMULATIONS



The simulations have been carried out in ANSYS FLUENT using finite difference method (FDM) technique. The air-water interface has been captured using an interface tracking technique known as Volume of Fluid (VOF) method.

A. Boundary Conditions

For solution of any CFD problem, boundary conditions have to be specified. Boundary conditions are thus important for a mathematical model. They direct the motion of flow which form a unique solution. Boundary conditions for the present study are as in Table 1.

TABLE 1

BOUNDARY CONDITIONS

Sl. No.	Boundary	Type
1	Inlet	Symmetry
2	Outlet	Pressure outlet
3	Top, bottom	Zero shear
4	Overset	Overset
5	Wing	No-slip

B. Solver Settings

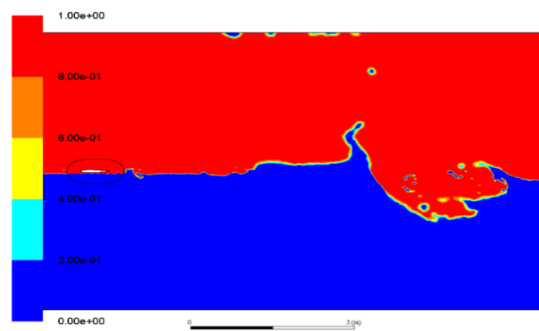
The inner domain was given a forward translation in negative x direction, with a forward velocity of $V=30$ m/s. The time-step size chosen is $\Delta t = 0.0001$, calculated by satisfying the CFL criterion and each simulations were carried out for 5000 time steps.

IV. RESULTS AND DISCUSSIONS

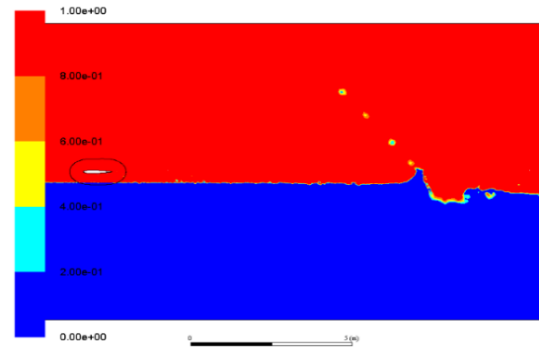
A. Estimation of optimum h/c .

The simulations result shows free surface deformations due to the aero-hydrodynamic interactions when the wing moves in close proximity to the surface of the water. The simulations were carried out for both in-ground effect (IGE) and out of ground effect (OGE). The starting vortex is well captured in downstream side. The undulations are heavier for simulations with in-ground effects and it is very high for $h/c=0.1$. These undulations reduce as h/c increases so that less deformations are occurred for simulations with out of ground effect. Fig. 4 shows the free-surface deformations and undulations for different values of h/c .

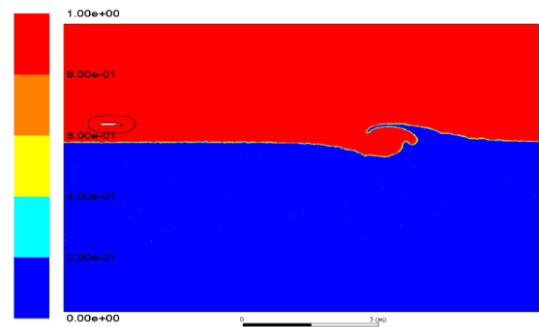
The lift to drag coefficient ratio C_L/C_D is observed to increase with increase in ground clearance till $h/c=0.3$ and then reduces when the wing has entered OGE conditions. So that the optimum h/c ratio is selected as 0.3, which is 0.3c height from the water surface. Variation of drag coefficient C_D with deformable ground effect for NACA0012 is shown in Fig. 5, variation of lift coefficient C_L with deformable ground effect is shown in Fig. 6, and variation of L/D with deformable ground effect is shown in Fig. 7.



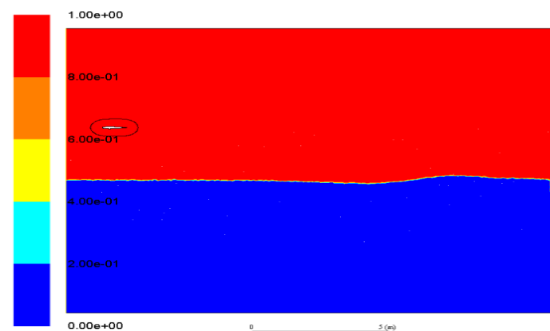
(a) $h/c=0.1$



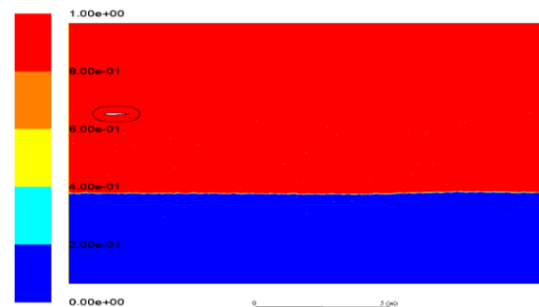
(b) $h/c=0.4$



(a) $h/c=1.0$



(a) $h/c=3.0$



(a) $h/c=5.0$

Fig. 4



Aero-hydrodynamic interactions for NACA0012 at various h/c .

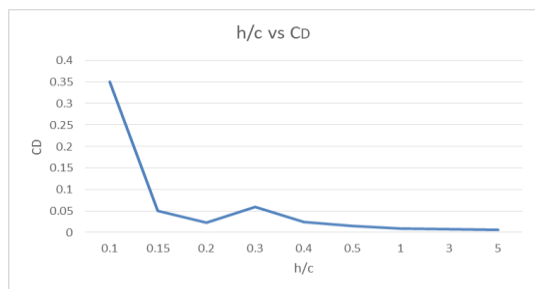


Fig. 5 Variation of drag coefficient C_D with h/c for NACA0012

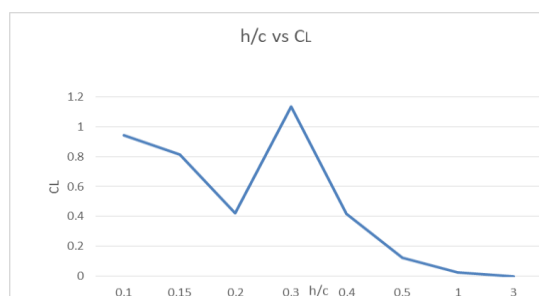


Fig. 6 Variation of lift coefficient C_L with h/c for NACA0012

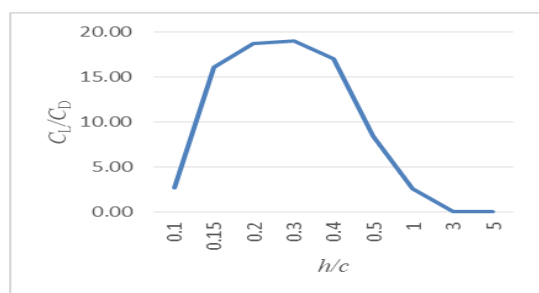
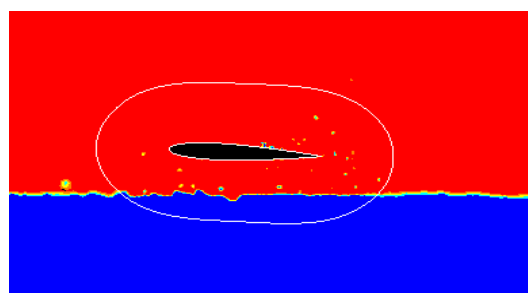
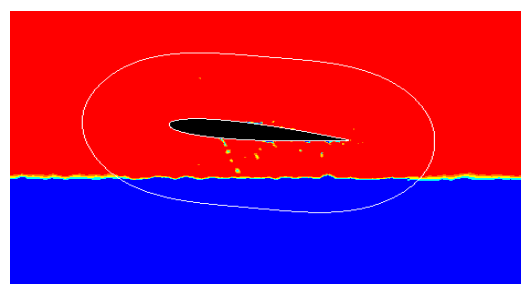


Fig. 7 Variation of L/D with h/c for NACA0012

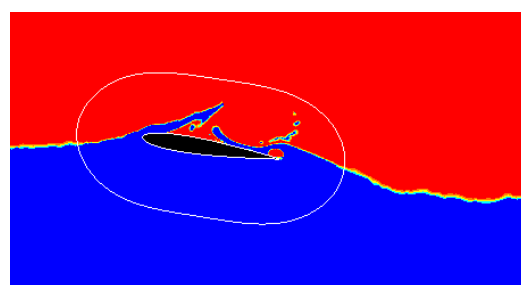
Preliminary studies were carried out on the effect of angle of attack (α) on lift-to-drag ratio for $h/c \geq 0.3$. The aero-hydrodynamic interactions for $3^\circ \leq \alpha \leq 9^\circ$ are shown in Fig. 8. As the angle of attack increases, lift force increases but the moisture dispersion around the wing is also observed to be increasing. Because of this denser fluid envelope, additional drag which is known as secondary drag will become predominant. Hence for lower h/c values a drop in L/D is observed at higher angles of attack (Fig. 9).



(a) $\alpha = 3^\circ$



(b) $\alpha = 6^\circ$



(c) $\alpha = 9^\circ$

Fig. 8 Aero-hydrodynamic interactions for various α at optimum $h/c=0.3$

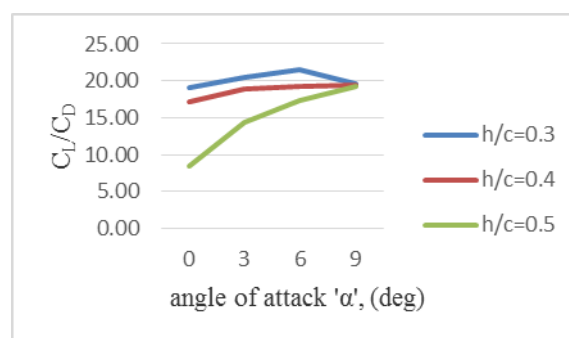


Fig. 9 Variation of L/D with α for $h/c \geq 0.3$

B. Structural Analysis at optimum h/c

The structural analysis helps to determine the cause of structural failure of a body. In static structural analysis, steady loading and response conditions are assumed; that is, the loads and the structure's response are assumed to vary slowly with respect to time. It is done in the ANSYS Workbench.

The wing is modeled in ANSYS Workbench. The material used for the structure is aluminum alloys. Aluminum alloys don't corrode as readily as steel. It has also been used for the skin of some high-speed airplanes, because it shows higher strength at higher temperatures. The model is meshed and it has given fixed support at one end. The lift force (625.12 kN) for 0.3 h/c ratio which is obtained from 2D simulation is applied at the bottom surface. The total deformation, von mises stress or equivalent stress, maximum principal stress, stress intensity, maximum shear stress and shear stress of wing are computed from the structural analysis. The maximum deformation occurs at the wing tip and it lowers



towards the fixed support. The stresses are maximum at the fixed support.

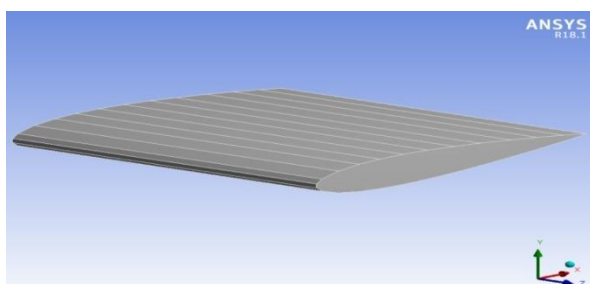


Fig. 10 Wing modeled in ANSYS Workbench

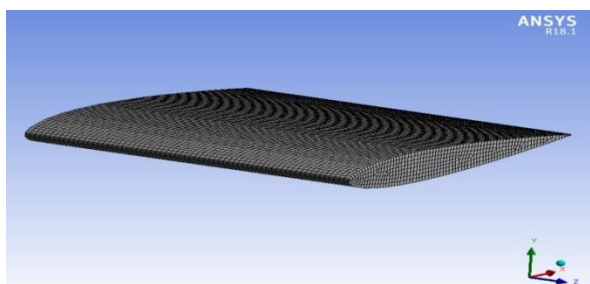


Fig.11 Meshed diagram of wing

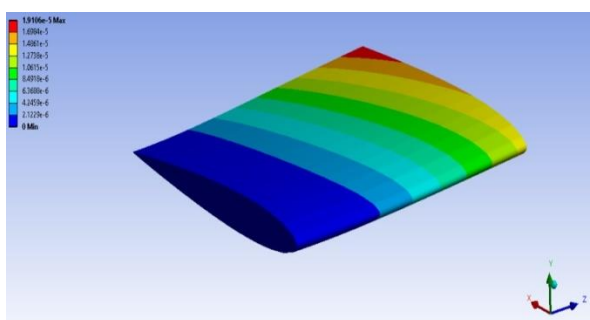


Fig. 12 Total Deformation of the wing

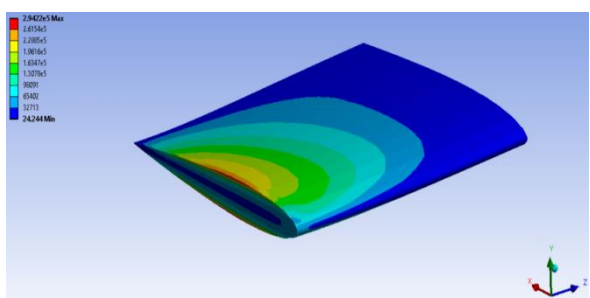


Fig. 13 Von misses stress distribution of the wing

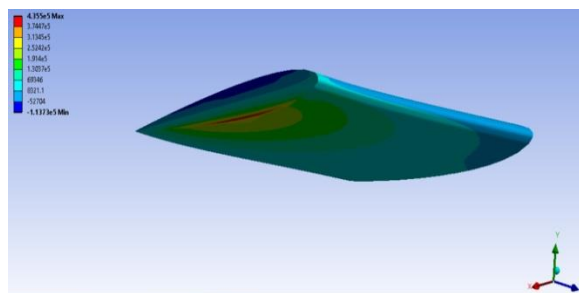


Fig. 14 Maximum principal stress distribution of the wing

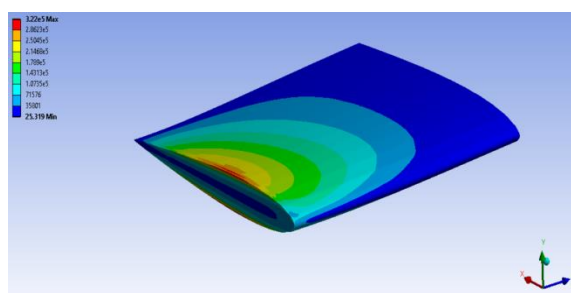


Fig. 15 Stress intensity of the wing

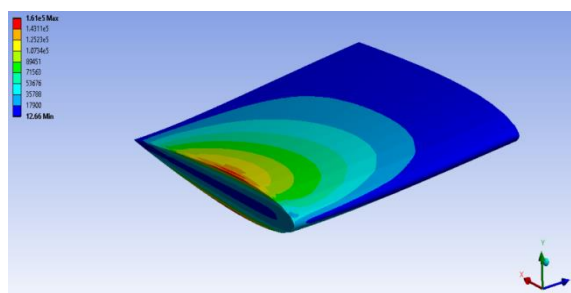


Fig. 16 Maximum shear stress distribution of the wing

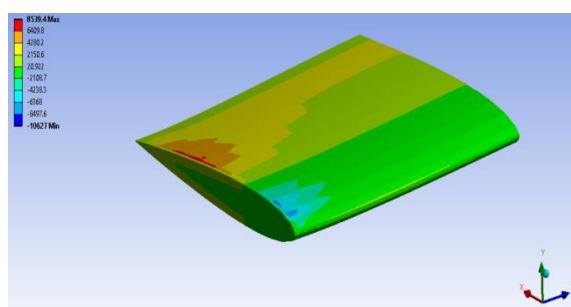


Fig. 17 Shear stress distribution of the wing

The deflection obtained from structural solver have been verified using cantilever deflection equation for uniformly distributed load given by Eq. (1)

$$\delta_{\max} = \frac{wl^4}{8EI} \quad (1)$$

Here δ_{\max} is the deflection, w is the load, l is the length of wing, E is the young's modulus and I is the Moment of Inertia. The value obtained is 0.018mm. It shows a deviation of 5.5%. The deformation and stress values obtained from



structural analysis is shown in Table 2.

TABLE 2

DEFORMATION AND STRESS VALUES

Sl. No.		Maximum Value	Minimum Value
1	Total Deformation (mm)	0.019	0
2	Von misses stress (N/mm ²)	0.294	2.424e-5
3	Maximum principal stress (N/mm ²)	0.435	-0.114
4	Stress intensity (N/mm ²)	0.322	1.266e-5
5	Maximum shear stress(N/mm ²)	0.161	2.532e-6
6	Shear stress(N/mm ²)	8.539e-3	-0.011

The computed stresses from the structural solver can be validated using bending equations. Bending stress and shear stress can be calculated using the Eq. (2) and (3) as given below:

$$\sigma_b = \frac{My}{I} \quad (2)$$

$$\tau = \frac{6F}{bd^3} \left[\frac{d^2}{4} - y^2 \right] \quad (3)$$

Where σ_b is the bending stress, M is the bending moment, y is the vertical distance away from the neutral axis, τ is the shear stress, b is the width of the beam, d is the depth. The bending stress value is 0.28 N/mm² and shear stress value is 0.008 N/mm², which shows a deviation of 6%. Using these values we can calculate von misses stress, maximum principal stress and maximum shear stress. Von misses stress equation is given by Eq. (4).

$$\sigma_v = \sqrt{\sigma_b^2 + \tau^2} \quad (4)$$

σ_v is the von misses stress, shear force will be zero at y_{max} . The calculated value is 0.28 N/mm², which shows 3.5% deviation. Maximum principal stress equation is as in Eq. (5)

$$P_1 = \frac{\sigma_1 + \sigma_2}{2} + \sqrt{\left(\frac{\sigma_1 + \sigma_2}{2}\right)^2 + \tau^2} \quad (5)$$

P_1 is the maximum principal stress and the value obtained is 0.39 N/mm², shows 10% deviation. Maximum shear stress equation is represented by Eq. (6).

$$q = \sqrt{\left(\frac{\sigma_1 + \sigma_2}{2}\right)^2 + \tau^2} \quad (6)$$

Where q is the maximum shear stress. The value obtained is 0.15 N/mm² and it shows a deviation of 6.6%.

V. CONCLUSIONS

A detailed numerical investigation on structural behavior of wing in deformable ground effect of a seaplane has been carried out using CFD simulations. The optimum h/c ratio for the effective operation of seaplane is obtained at 0.3. The structural behavior of NACA0012 symmetric wing shows less deformation at the optimum flying conditions. The maximum deformation of wing occurs at the wing tip and the stresses are maximum at the fixed support. These results show efficient aero-hydrodynamic performance of seaplane hence, translates into fuel saving. This method presented in this piece of work provides some insights into the structural behavior of a wing subjected to maximum aero-hydro interaction.

REFERENCES

1. S Gudmundsson, "APPENDIX C3: Design of Seaplanes", General Aviation Aircraft Design: Applied Methods and Procedures, Elsevier, Inc., 2013.
2. M.M. Tofa, A Maimun, Y.M. Ahmed, S Jamei and A Priyanto, Rahimuddin, "Experimental Investigation of a Wing-in-Ground Effect Craft", The Scientific World Journal, Vol. 2014, Article ID 489308, 2014.
3. A.K. Arumugham-Achari, S. Janardhanan, R.P. Nair and A. Jose, "Numerical Investigations on the Wing-in-Deformable Ground Effect for Seaplanes", International Conference on Computational and Experimental Marine Hydrodynamics, 2018.
4. B.C. Khoo and H.B. Koe, "The hydrodynamics of the WIG (Wing-In-Ground) Effect Craft", IEEE 6th International Conference on Underwater System Technology: Theory & Applications, 2016.
5. M Tavakoli and M Saeed Seif, "A Practical Method for Investigation of Aerodynamic and Longitudinal Static Stability of Wing-in-Ground Effect", International Journal of Maritime Technology, Vol.4/Summer (11-19), 2015.
6. W.M. Chan, R.J. Gomez III, S.E. Rogers, P.G. Buning, "Best Practices In Overset Grid Generation", 32nd AIAA Fluid Dynamics Conference, 2002.
7. Rajesh, M., and J. M. Gnanasekar. "Path Observation Based Physical Routing Protocol for Wireless Ad Hoc Networks." Wireless Personal Communications 97.1 (2017): 1267-1289.
8. Rajesh, M., and J. M. Gnanasekar. "Sector Routing Protocol (SRP) in Ad-hoc Networks." Control Network and Complex Systems 5.7 (2015): 1-4.
9. Rajesh, M. "A Review on Excellence Analysis of Relationship Spur Advance in Wireless Ad Hoc Networks." International Journal of Pure and Applied Mathematics 118.9 (2018): 407-412.
10. Rajesh, M., et al. "SENSITIVE DATA SECURITY IN CLOUD COMPUTING AID OF DIFFERENT ENCRYPTION TECHNIQUES." Journal of Advanced Research in Dynamical and Control Systems 18.
11. Rajesh, M. "A signature based information security system for vitality proficient information accumulation in wireless sensor systems." International Journal of Pure and Applied Mathematics 118.9 (2018): 367-387.
12. Rajesh, M., K. Balasubramaniaswamy, and S. Aravindh. "MEBCK from Web using NLP Techniques." Computer Engineering and Intelligent Systems 6.8: 24-26.